Functional insight into the role of Orc6 in septin complex filament formation in *Drosophila*

Katarina Akhmetova[a,b], Maxim Balasov[a], Richard P. H. Huijbregts[a,*], and Igor Chesnokov[a]
[a]Department of Biochemistry and Molecular Genetics, University of Alabama at Birmingham School of Medicine, Birmingham, AL 35294; [b]Institute of Cytology and Genetics, Novosibirsk 630090, Russia

ABSTRACT **Septins belong to a family of polymerizing GTP-binding proteins that are important for cytokinesis and other processes that involve spatial organization of the cell cortex. We reconstituted a recombinant *Drosophila* septin complex and compared activities of the wild-type and several mutant septin complex variants both in vitro and in vivo. We show that *Drosophila* septin complex functions depend on the intact GTP-binding and/or hydrolysis domains of Pnut, Sep1, and Sep2. The presence of the functional C-terminal domain of septins is required for the integrity of the complex. *Drosophila* Orc6 protein, the smallest subunit of the origin recognition complex (ORC), directly binds to septin complex and facilitates septin filament formation. Orc6 forms dimers through the interactions of its N-terminal, TFIIB-like domains. This ability of the protein suggests a direct bridging role for Orc6 in stimulating septin polymerization in *Drosophila*. Studies reported here provide a functional dissection of a *Drosophila* septin complex and highlight the basic conserved and divergent features among metazoan septin complexes.**

Monitoring Editor
Daniel J. Lew
Duke University

Received: Feb 10, 2014
Revised: Oct 14, 2014
Accepted: Oct 17, 2014

INTRODUCTION

The septins are highly conserved guanine nucleotide–binding, filament-forming proteins found in a majority of eukaryotic organisms. They localize primarily to the cell membranes and participate in many cellular processes, including cytokinesis, cell movement and polarity, ciliogenesis, secretion, cell–pathogen interaction, and cytoskeletal dynamics (Kinoshita, 2006; Weirich *et al.*, 2008; Estey *et al.*, 2011; Saarikangas and Barral, 2011; Mostowy and Cossart, 2012). In most cases, septins function as scaffolds to recruit and maintain the localization of other proteins or serve as membrane diffusion barriers compartmentalizing discrete cellular domains (Longtine *et al.*, 1998, 2000; Field and Kellogg, 1999; Barral *et al.*, 2000; Takizawa *et al.*, 2000; Caudron and Barral, 2009; Saarikangas and Barral, 2011; Hall and Russell, 2012). The considerable diversity of biological processes served by septins is based on the ability of these proteins to form complexes and filaments.

Septins belong to the GTPase superclass of phosphate-binding loop (P-loop) NTPases (Leipe *et al.*, 2002). Most of the septins possess a central GTP-binding (G) domain with a set of conservative GTPase motifs flanked by variable N- and C- termini (NC), where the C-terminus is predicted to form a coiled-coil domain. Within the G-domain, the diphosphate-binding loop (P-loop or G-1 motif) with the consensus sequence GxxGxGKST contacts the α- and β-phosphates of the guanine nucleotide, G-3 motif (DxxG) participates in binding of Mg^{2+} and the γ-phosphate of GTP, and G-4 motif (xKxD) is responsible for the recognition of the guanine ring (Sprang, 1997). Even though GTP-binding and GTP-hydrolyzing activities of the purified and recombinant septin complexes or polypeptides have been demonstrated in vitro, the biochemical and biological significance of septin GTPase activity remains unclear (Field *et al.*, 1996; Kinoshita *et al.*, 1997; Mendoza *et al.*, 2002; Casamayor and Snyder, 2003; Weirich *et al.*, 2008). Structural studies and functional analysis of septins performed in recent years (Vrabioiu *et al.*, 2004; Sirajuddin *et al.*, 2007, 2009; Zent *et al.*, 2011; Wittinghofer and Zent, 2014) strongly suggest that the purpose of having different nucleotide states in septins is to allow structural transitions and recycling of septin filaments during particular stages of the cell cycle. Conserved interactions between adjacent GTPase domains and/or the NC-terminal extensions of septins appear to be important for the formation of heteromeric complexes that can further polymerize

This article was published online ahead of print in MBoC in Press (http://www.molbiolcell.org/cgi/doi/10.1091/mbc.E14-02-0734) on October 29, 2014.

*Present address: Department of Pathology, University of Alabama at Birmingham, Birmingham, AL 35233.

Address correspondence to: Igor Chesnokov (ichesnokov@uab.edu).

Abbreviations used: CTD, C-terminal domain; GTPγS, guanosine 5′-*O*-(3-thiotriphosphate); ORC, origin recognition complex.

into filaments (Sirajuddin *et al.*, 2007; Wittinghofer and Zent, 2014). The ability of septins to form filaments has been shown to be crucial for septin functioning in cellular processes (Sheffield *et al.*, 2003; Sirajuddin *et al.*, 2009; McMurray *et al.*, 2011); however, factors responsible for the regulation of septin filament formation are not well understood.

Drosophila melanogaster has five septin proteins—Pnut, Sep1, Sep2, Sep4, and Sep5. Of these septins, Pnut, Sep1, and Sep2 form a heteromeric six-subunit complex consisting of two of each septin subunit (Field *et al.*, 1996). Septin proteins in *Drosophila* associate with membranes of the cellularization front, with membranes of imaginal disks, larval CNS, photoreceptor cells, and ring canals (Neufeld and Rubin, 1994; Fares *et al.*, 1995; Hime *et al.*, 1996; Adam *et al.*, 2000; Kinoshita, 2003). The complex of Pnut, Sep1, and Sep2 binds and hydrolyzes GTP, but the significance of septin GTPase activity in cells is poorly understood (Field *et al.*, 1996). GTP binding by septins appears to be important for filament formation; however, additional factors, including interacting proteins, probably regulate the dynamics of septin polymerization in vivo.

In our earlier studies (Chesnokov *et al.*, 2001, 2003), we established that the smallest subunit of the origin recognition complex (ORC), Orc6 protein, is important for cytokinesis in *Drosophila* and has an active role in septin complex functions. The ORC plays a central role in the initiation of DNA replication but is also involved in nonreplicative functions (Bell, 2002; Bell and Dutta, 2002; Machida *et al.*, 2005; Chesnokov, 2007). Orc6 protein is necessary for DNA replication function in all eukaryotes (Semple *et al.*, 2006; Balasov *et al.*, 2007; Chen *et al.*, 2007; Sasaki and Gilbert, 2007). Metazoan Orc6 proteins consist of two functional domains: a larger N-terminal domain important for binding of DNA, and a smaller C-terminal domain important for protein–protein interactions (Chesnokov *et al.*, 2003; Balasov *et al.*, 2007; Duncker *et al.*, 2009; Bleichert *et al.*, 2013). It has been shown that in metazoan species, the N-terminal domain of Orc6 carries a structural homology with TFIIB transcription factor (Chesnokov *et al.*, 2001; Balasov *et al.*, 2007; Liu *et al.*, 2011). The conserved motif in the C-terminus is responsible for the interaction with the Orc3 subunit of ORC, and mutations in this region of the protein are linked to the Meyer–Gorlin syndrome in humans (Bleichert *et al.* 2013).

Orc6 is also essential for cytokinesis in both *Drosophila* and human cells (Prasanth *et al.*, 2002; Chesnokov *et al.*, 2003; Balasov *et al.*, 2007; Liu *et al.*, 2011). In *Drosophila*, Orc6 colocalizes and interacts with the septin protein Pnut (Chesnokov *et al.*, 2003; Huijbregts *et al.*, 2009). This interaction is mediated by C-terminus of Orc6, which contains a predicted amphipathic α-helical domain and C-terminal coiled-coil domain of Pnut protein (Chesnokov *et al.*, 2003; Huijbregts *et al.*, 2009). We observed earlier that Orc6 stimulates septin complex GTPase activity and polymerization during filament assembly and hypothesized that Orc6 might stabilize septin filaments through protein–protein interactions (Huijbregts *et al.*, 2009).

In this work we analyzed the detailed roles of conserved septin motifs, GTP, and Orc6 in septin complex functions both in vitro and in vivo in a live animal. We used recombinant wild- type and mutant *Drosophila* septins to investigate the requirements for GTP binding/hydrolysis by Pnut, Sep1, and Sep2 in septin complex functions, as well as the role of Orc6 in septin complex polymerization. Our work represents in vitro and in vivo analyses of the septin complex in *Drosophila*, showing the importance of functional septin complex in *Drosophila* development.

RESULTS

GTPase activity of individual septin proteins

To study GTPase activity, we isolated recombinant wild-type and mutant septin proteins and purified them using an *Escherichia coli* expression system. The wild-type and mutant proteins used in this study are presented in Figure 1A and Supplemental Figure S1, A and B. First, individual septin proteins were analyzed for GTP incorporation and hydrolysis (Table 1). Both wild-type Pnut and Sep1 proteins displayed robust GTPase hydrolysis and readily incorporated GTP. Sep2 protein, on the other hand, did not possess any noticeable GTPase activity (Table 1). These results are in agreement with previously reported studies on human septin complex (Sirajuddin *et al.*, 2007), in which SEPT7 and SEPT2 (homologues of *Drosophila* Pnut and Sep1 respectively) were found in GDP-bound forms, and SEPT6 (*Drosophila* Sep2) contained GTP nucleotide. Earlier studies on *Drosophila* septin complex also suggested that Sep2 does not exchange bound GTP (Field *et al.*, 1996). To address the role of GTP in *Drosophila* septin complex activities, we next introduced single as well as triple mutations into G1, G3, and G4 motifs of the GTPase domain of Pnut, Sep1, and Sep2 (Figure 1A and Supplemental Figure S1, A and B). The levels of GTP incorporation and hydrolysis by individual mutant

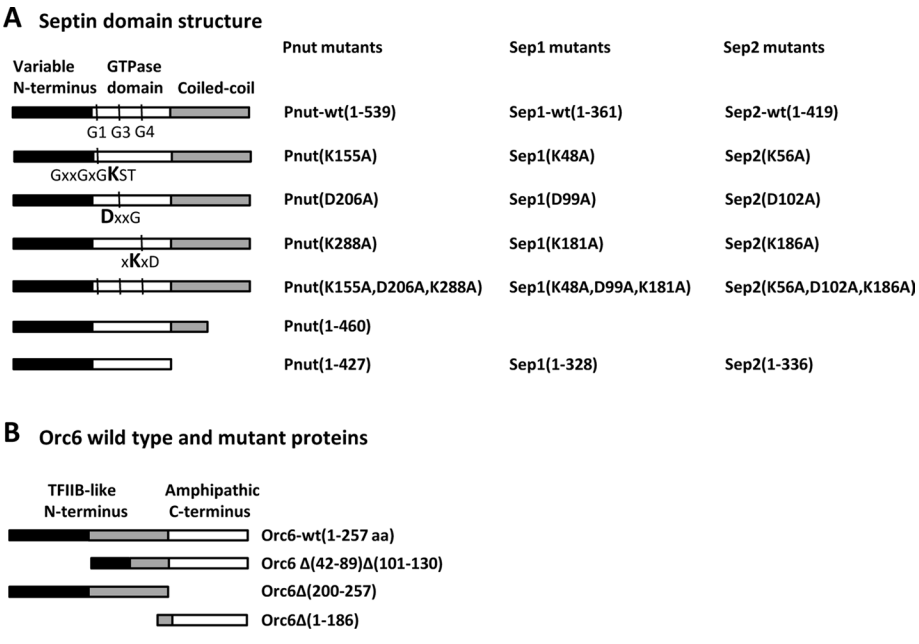

FIGURE 1: Recombinant proteins used in this study. (A) Wild-type and mutant septin proteins used in this study. Left, schematic representation of septin structure. Right, mutations in conserved domains for each septin protein. Conservative amino acid residues in G1, G3, and G4 motifs of septin GTPase domain (boldface) were replaced with alanines. (B) Wild-type and mutant Orc6 proteins used in this study. Orc6-wt (1–257), full-size wild-type Orc6; Orc6 Δ(42–89)Δ(101–130), Orc6 missing parts of two globular TFIIB-like domains; Orc6 Δ(200–257), Orc6 with truncated C-terminus; Orc6 Δ(1–186), N-terminus deletion. First and second globular domains are shown in black and gray, respectively.

Septin	Incorporation (mol GTP/mol protein)	GDP (fraction of total nucleotide)
His-Pnut	0.02787 ± 0.00061	0.86 ± 0.12
His-Pnut(G1)	0.00013 ± 0.00023	0.39 ± 0.04
His-Pnut(G3)	0.00024 ± 0.00029	0.64 ± 0.22
His-Pnut(G4)	0.00014 ± 0.00024	0.31 ± 0.06
His-Pnut(G1,G3,G4)	0.00017 ± 0.00022	0.51 ± 0.03
His-Pnut(1-460)	0.05284	0.97 ± 0.01
His-Pnut(1-427)	0.03532	0.97 ± 0.01
His-Sep1	0.06935 ± 0.01087	0.99 ± 0.01
His-Sep1(G1)	0.00117 ± 0.00150	0.23 ± 0.12
His-Sep1(G3)	0.00077 ± 0.00013	0.30 ± 0.16
His-Sep1(G4)	0.00136 ± 0.00039	0.50 ± 0.06
His-Sep1(G1,G3,G4)	0.00222 ± 0.01800	0.16 ± 0.02
Sep2	0.00036	0.05

GTP incorporation adjusted after background subtraction and the amount of bound nucleotide converted to GDP for individual septin proteins are shown (mean ± SD). Background is the amount of radioactivity bound to the filter for the sample without protein. GTPase assays were performed in triplicate, except for His-Pnut(1–460), His-Pnut(1–427), and Sep2, for which the average of two experiments is shown. *p* values were determined with Student's *t* test (relative to the wild type for each mutant); $p < 0.05$ except for the His-Pnut(G3) GDP fraction, for which $p = 0.38$.

TABLE 1: GTPase activity of recombinant individual septins.

septin proteins were measured and are presented in Table 1. For all G-domain mutants, GTP incorporation levels were significantly lower than with the wild-type proteins. GTP hydrolysis was also reduced for all tested mutants. Because Sep2 protein does not exchange bound GTP, corresponding mutations did not have any noticeable effect on the activities of this particular protein (unpublished data). Of interest, deletions of Pnut coiled-coil C-terminal domain (CTD) resulted in increased incorporation of GTP and GTP hydrolysis. A similar effect was observed in *Saccharomyces cerevisiae*, in which a truncated version of Cdc12 with the deletion of the coiled-coil domain displayed a rate of GTP hydrolysis fourfold to fivefold higher than that of full-length Cdc12 (Versele and Thorner, 2004).

Analysis of septin complex assembly using septin mutants

An important characteristic of septins is their ability to form heteromeric complexes with each other. It was shown previously that *Drosophila* septins Pnut, Sep1, and Sep2 form a six-subunit complex consisting of two of each septin subunit (Field *et al.*, 1996). To define the importance of GTPase motifs for complex formation, we expressed wild-type septin proteins and septin mutants carrying mutations in GTPase domain simultaneously, using a baculovirus expression system to reconstitute septin complexes. Histidine (His) tag was added to the N-terminus of Pnut protein to facilitate complex purification. As presented in Supplemental Figure S1C, Pnut and Sep1 carrying single GTPase mutations (in the G1, G3, or G4 motif) were able to reconstitute into septin complex. Pnut carrying a triple GTPase mutation was also able to enter the complex (Supplemental Figure S1C, lane 9). However, similar triple mutations in Sep1 resulted in inability of this mutant to form a complex with other septins (Supplemental Figure S1C, lane 10), indicating the importance of these motifs in Sep1 for the integrity of the whole complex. Similar mutations in the Sep2 GTPase motif also resulted in diminished association of Sep1 with the rest of the complex (Supplemental Figure S1C, lane 11), supporting a structural rather than regulatory role for Sep2 in *Drosophila* septin complex assembly, as was also proposed for SEPT6 in human septin complex (Sirajuddin *et al.*, 2007).

In contrast to the studies of human septin complex (Sirajuddin *et al.*, 2007), we found that deletions of C-terminal motifs of *Drosophila* Pnut prevented septin complex formation (Huijbregts *et al.*, 2009). Furthermore, the complex did not form when deletions of C-terminal domains were introduced into all septins (Pnut, Sep1, and Sep2) constituting *Drosophila* septin complex (Supplemental Figure S2).

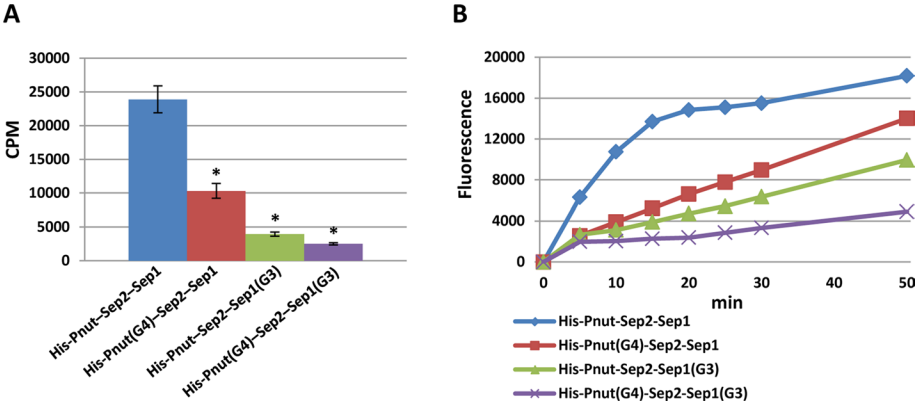

FIGURE 2: GTPase activity of recombinant septin complexes. (A) GTP binding of recombinant septin complexes. Recombinant septin complexes (wild type or mutant) were incubated with 5 μCi of [α-^{32}P]GTP and 2 μM cold GTP for 1 h and applied to a 0.22-μm membrane. Membranes were washed, air dried, and counted in a liquid scintillation counter. Values represent the average cpm counts minus the background (control reaction without the addition of the complex). Error bars represent SD; asterisk indicates significantly different from wild type (Student's *t* test, $p < 0.05$), $n = 5$. (B) GTP hydrolysis of recombinant septin complexes. Recombinant septin complexes (wild type or mutant) were incubated with 100 μM GTP in the presence of phosphate sensor (Invitrogen), a phosphate-binding protein modified with a fluorophore. As the sensor binds free phosphate, its fluorescence increases. Values represent fluorescence emission intensities at time points indicated for a representative experiment. Background (value at zero time point) was subtracted from all measured values.

GTPase activity of mutant septin complexes

Next, septin complexes carrying Pnut and Sep1 GTPase mutants (Supplemental Figure S1C) were analyzed in reactions of GTP binding (Figure 2A) and hydrolysis (Figure 2B). For this analysis, we selected Pnut and Sep1 mutants with the most profound effect on GTPase activity. As shown in Figure 2, mutation in the G4 domain of Pnut resulted in twofold to threefold decrease in both GTP binding and hydrolysis for the septin complex that contained this mutant. Mutations in the G3 motif of Sep1 had a significantly stronger effect, resulting in fourfold to sixfold decrease in complex activities. The complex carrying double mutations for both Pnut (G4) and Sep1 (G3) had the most dramatic effect, and prolonged incubation of this complex with GTP did not improve either GTP incorporation or hydrolysis (Figure 2, A and B). We conclude that the in vitro GTPase activity of *Drosophila* septin complex consists of combined activity of Sep1 and, to a lesser extent, Pnut proteins.

The effect of GTP and Orc6 on septin filament formation

We previously reported that the addition of Orc6 had a stimulatory effect on septin polymerization (Huijbregts *et al.*, 2009). Moreover, we observed that the addition of GTP resulted in disassembly of septin filaments when low concentrations of the nucleotide were used in reactions (Huijbregts *et al.*, 2009). Here we tested the effects of increasing concentrations of GTP, as well as the addition of wild-type Orc6, on filament formation by wild-type and mutant septin complexes. Filament formation was visualized and monitored using negative-stain electron microscopy (EM). The concentration of recombinant septin complex was adjusted in such a way as to visualize individual septin hexameric complexes under the conditions used for EM (Supplemental Figure S3 and Figure 4A later in this article). No noticeable effect was observed when GTP was added to the reactions containing relatively low (~10 ng/μl) concentrations of septin complex (Supplemental Figure S3). Substitution of GTP with GDP or GTPγS (nonhydrolyzable analogue of GTP) also had no effect (Supplemental Figure S3). Increasing the concentration of septin complex and/or addition of crowding agents such as polyethylene glycol resulted in a formation of large, cable-like filaments (unpublished data). The concentration dependence of septin complex solutions to form larger aggregates was also described previously and involves a lateral association of the filaments (Field *et al.*, 1996; Huijbregts *et al.*, 2009).

In agreement with previous data (Huijbregts *et al.*, 2009), the addition of Orc6 greatly enhanced filament formation (Figure 3A). As we reported previously (Huijbregts *et al.*, 2009), the addition of low concentration (~2 μM) of GTP resulted in the disassembly of the filaments. Here we also observed that in the presence of low GTP concentrations, filaments had a tendency to dissociate easily. Two representative images are presented in Figure 3A, top. Increasing concentrations of GTP further toward saturation reproducibly resulted in longer and more pronounced septin filaments in the presence of Orc6 (Figure 3A). These results suggest that low concentrations of GTP reported in earlier publications (Field *et al.*, 1996; Huijbregts *et al.*, 2009) may result in the depletion of GTP during reactions and premature disassembly of filaments as detected by EM. The addition of GDP and GTPγS also resulted in septin polymerization (Figure 3A, bottom; Huijbregts *et al.*, 2009). However, careful estimation of the filament length revealed statistically significant increase in the length of septin filaments formed in the presence of 1 mM GTP and Orc6 compared with the filaments formed in the presence of either 1 mM GDP or 1 mM GTPγS with added Orc6 (Figure 3B and Supplemental Table S1).

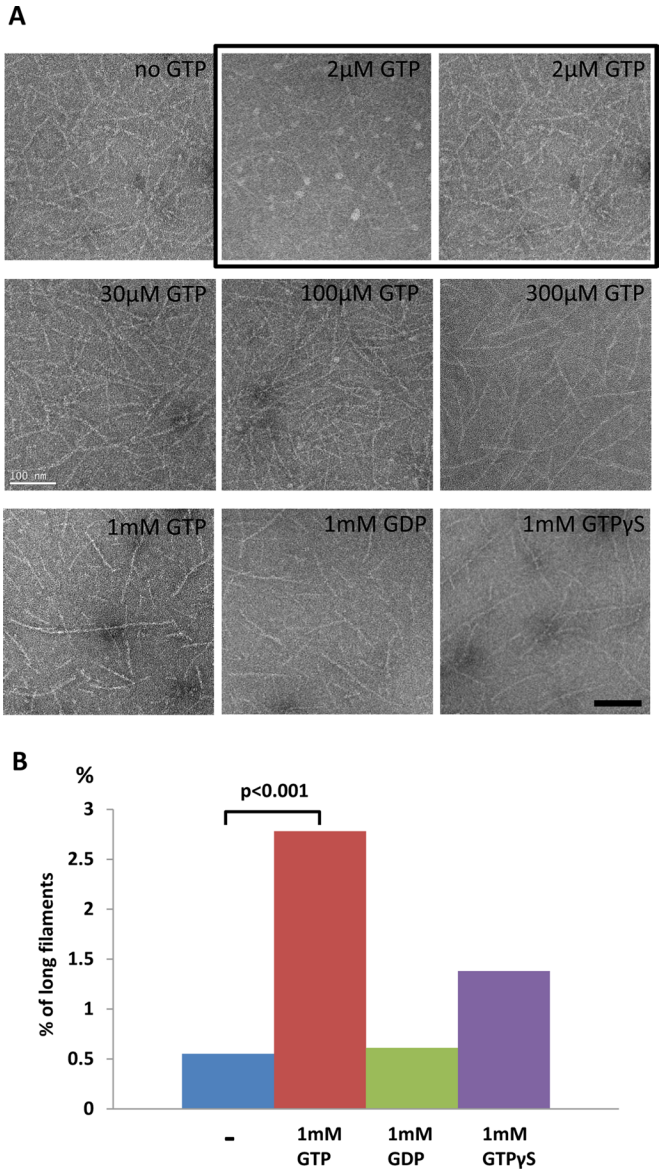

FIGURE 3: The effect of guanine nucleotides on septin filament formation in the presence of Orc6. (A) Recombinant wild-type septin complex His-Pnut-Sep2-Sep1 (10 ng/μl) was incubated without any nucleotide or with different concentrations of GTP, GDP, or GTPγS (as indicated) in the presence of Orc6 (15 ng/μl). Samples were incubated for 2 h at room temperature (22°C) and then visualized by negative-stain transmission EM. Scale bar, 100 nm. (B) Percentage of long filaments (composed of ≥10 septin complex monomers) for the reactions of septin filament formation shown in A. $p < 0.001$ (chi-square test) as indicated. Complete data and statistical analysis are presented in Supplemental Table S1.

Filament formation of septin complexes containing septins with GTPase mutations

To further investigate the role of GTPase domain in septin filament formation, we analyzed the ability of septin complexes with mutated GTPase domain motifs of Pnut, Sep1, and Sep2 to form filaments in vitro in the presence or absence of Orc6. Orc6 interacts with Pnut through its C-terminal domain, and mutations in Pnut GTPase motifs did not have any noticeable effect on interaction between Orc6 and Pnut (Supplemental Figure S4). In the absence of Orc6 we did not observe septin complex polymerization when GTPase mutants were used in reactions similar to the wild-type complex (Figure 4, A–D, first column). Low concentrations (~10 ng/μl) of septin complex were used for negative-stain EM to prevent concentration-dependent formation of septin polymers and aggregates. The addition of Orc6 had stimulating effect on filament formation of wild-type septin complex (Figure 4A); however, complexes carrying septin mutants displayed significantly reduced ability for polymerization in the presence of Orc6 and GTP (Figure 4, B–D). The representative results in Figure 4 are shown for the wild-type septin complex and complexes carrying Pnut (G4), Sep1 (G4), and Sep2 (G1, G3, G4) mutants.

In vivo analysis of Pnut mutants

Of all *Drosophila* septins, only the *pnut* deletion mutant has been identified and described (Neufeld and Rubin, 1994). Larvae homozygous null for *pnut* die soon after pupation, and *pnut*⁻ tissues fail to proliferate and instead develop clusters of large,

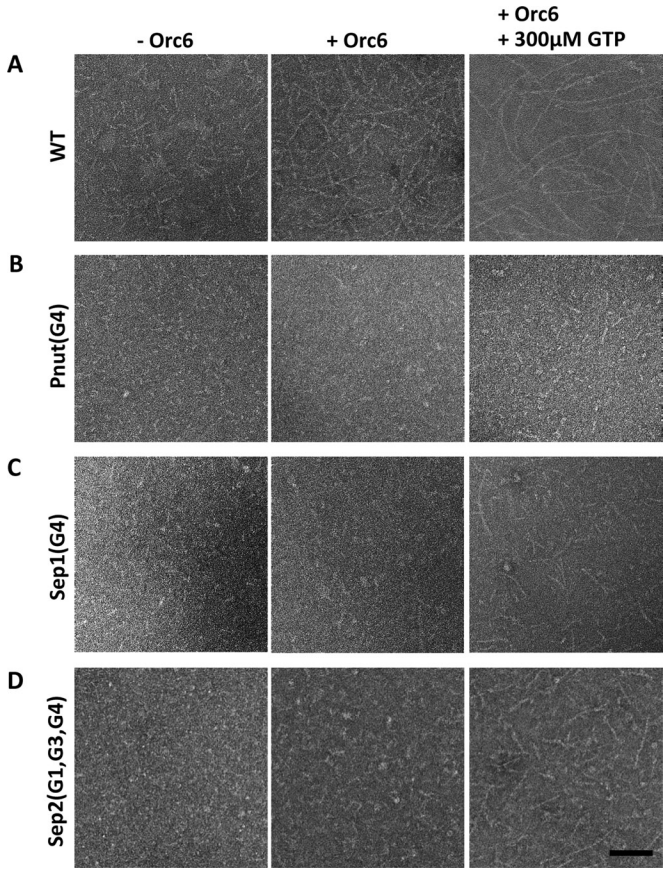

FIGURE 4: Mutations in septin GTPase domain result in defects of septin filament formation. Recombinant wild-type or mutant septin complex His-Pnut-Sep2-Sep1 (10 ng/μl) was incubated with or without Orc6 (15 ng/μl) in the absence or presence of 300 μM GTP as indicated. Wild-type septin complex (A) or complexes containing GTPase mutant Pnut(G4) (B), GTPase mutant Sep1(G4) (C), or triple GTPase mutant Sep2(G1,G3,G4) (D) were used. Samples were incubated for 2 h at 22°C and then visualized by negative-stain transmission EM. Scale bar, 100 nm.

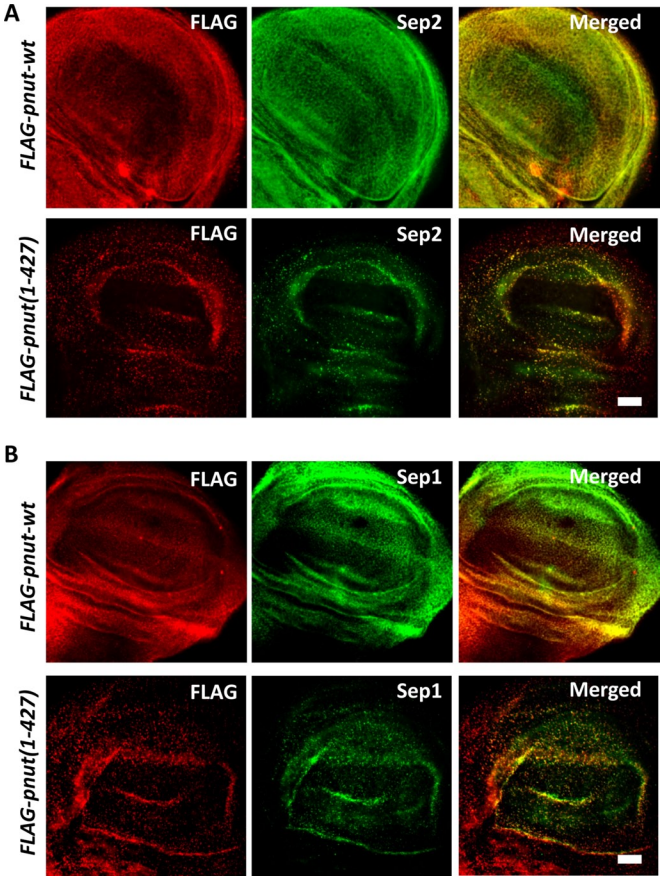

FIGURE 5: Pnut C-terminus deletion mutant forms aggregates in vivo and causes mislocalization of other septin proteins. *pnut*^{XP} null-allele mutant was rescued with wild-type *FLAG-pnut-wt* transgene or C-terminal deletion *FLAG-pnut(1-427)* transgene. Wing imaginal disks of third-instar larvae were immunostained for FLAG (red), showing FLAG-Pnut and either Sep2 (A) or Sep1 (B) (green) proteins. Scale bars, 10 μm.

multinucleated cells, indicating involvement of this protein in cytokinesis. We showed that the interaction of Orc6 with the septin complex is dependent on the C-terminal coiled-coil domain of Pnut (Huijbregts *et al.*, 2009). To study the effect of GTPase and CTD mutations of Pnut in vivo in live animals, we generated transgenic flies carrying corresponding mutant forms of Pnut. We used the *pnut*^{XP} null allele described by Neufeld and Rubin (1994). The introduction of transgenes carrying the C-terminal deletion of Pnut protein (amino acids 1–427; Figure 1A) did not rescue the *pnut*^{XP} third-instar lethal deletion; however, developing imaginal disks were found in such larvae, as compared with the disk-less phenotype of *pnut*^{XP} mutant larvae. Truncated Pnut protein did not show characteristic Pnut localization, as is shown in *FLAG-pnut-wt* rescue (Figure 5, A and B, top), instead forming mislocalized aggregates in developing imaginal disks (Figure 5, A and B, bottom) and in *Drosophila* L2 tissue culture cells (Huijbregts *et al.*, 2009). Of interest, both Sep1 and Sep2 proteins were also mislocalized in tissues carrying truncated Pnut (Figure 5, A and B). Furthermore, we found that ablation of Pnut due to RNA interference (RNAi) in *Drosophila* tissue culture cells also resulted in Sep1 mislocalization (Supplemental Figure S5). These results suggest that the integrity of the complex is required for proper localization of septin complex subunits in vivo.

Pnut transgenes carrying GTPase mutations were also not able to rescue flies to viability. Of interest, single G4 Pnut mutation, although lethal, did not lead to any visual defects in cytokinesis, as mutant larvae developed imaginal disks like wild-type flies, and no polyploidy mitoses were observed in neural ganglia (Figure 6A). However, when all three Pnut GTPase motifs (G1, G3, and G4) were mutated, larvae carrying this transgene had phenotype indistinguishable from that of null-allele homozygotes, such as the absence of imaginal disks and polyploidy metaphases in neural ganglia, as is shown in Figure 6, B and C. Further detailed analysis revealed the absence of characteristic intense "dot-like" Pnut localization on the membrane in *pnut*^{XP} larvae carrying *pnut* transgene with single G4 mutation in either imaginal disks or testes (Figure 7, C and F) as compared with the endogenous protein in *Canton S* flies (Figure 7, A and D) or *pnut*^{XP} flies rescued with wild-type *FLAG-pnut* transgene (Figure 7, B and E), even though diffuse staining at the membrane region was still observed. Our results suggest the importance of intact GTPase motifs in Pnut for proper protein localization in vivo and animal survival.

Orc6 associates stoichiometrically with septin filaments

Based on structural studies of human septins (Sirajuddin *et al.*, 2007) and sequence homologies between human and *Drosophila* septins (Pan *et al.*, 2007), septin complex can be described as a

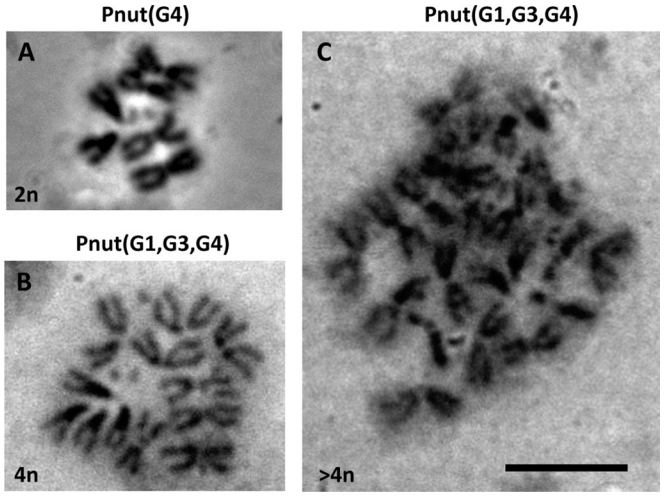

FIGURE 6: Mitoses in neural ganglia of Pnut GTPase domain mutants. (A) The 2*n* metaphases in *pnut*^{XP} mutant rescued with *FLAG-pnut (G4)* transgene. (B, C) Polyploid metaphases in *pnut*^{XP} mutant rescued with *FLAG-pnut (G1,G3,G4)* transgene with four (B) and more than four (C) sets of chromosomes. Scale bar, 10 μm.

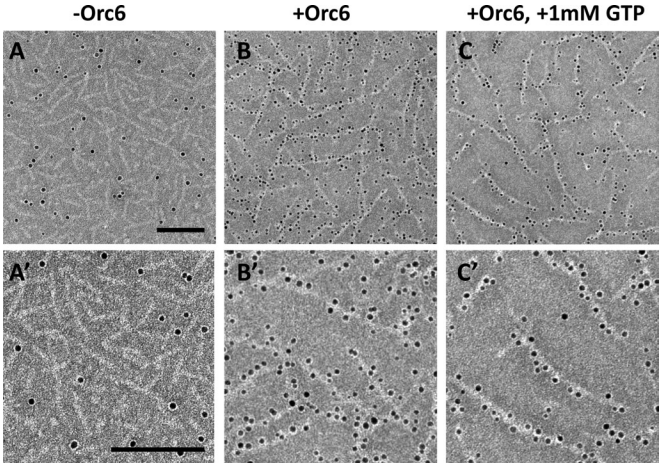

FIGURE 8: Orc6 directly interacts with septin filaments. Recombinant wild-type septin complex Pnut-Sep2-Sep1 (20 ng/μl) was incubated in the absence of His-Orc6 and any nucleotide (A, A'), in the presence of His-tagged Orc6 (15 ng/μl; B, B'), or in the presence of His-tagged Orc6 and 1 mM GTP (C, C'). After 2 h of incubation, samples were applied on EM grid and labeled with 5 nm Ni-NTA-Nanogold. Scale bars, 100 nm.

linear hexamer with Pnut protein at either end of the complex. We previously hypothesized (Huijbregts *et al.*, 2009) that Orc6 binding to Pnut may enhance linear filament assembly and stabilize the formation of the filaments by Orc6–Orc6 interactions. To look into the mechanism of Orc6's stimulating effect on septin polymerization, we first tried to visualize Orc6 in reactions of septin filament formation using negative-stain EM. We used nickel-nitriloacetic acid (Ni-NTA) Nanogold reagent, which binds specifically to His tag and allows visualization of His-tagged proteins during EM experiments. His tag was removed from purified recombinant septin complex, and the reaction of filament formation was set up in the presence of His-Orc6 and GTP. After a 2-h incubation, samples were applied on the EM grid and stained with Ni-NTA Nanogold to visualize His-Orc6. The results are presented in Figure 8. In the absence of Orc6, filaments were short, and Nanogold staining did not reveal any noticeable pattern (Figure 8, A and A'). However, the addition of His-tagged Orc6 greatly facilitated septin polymerization and allowed the detection of Orc6. As presented in Figure 8, B and B' (no GTP added), and Figure 8, C and C' (in the presence of GTP), His-Orc6 molecules specifically localize along septin filaments, consistent with a role for Orc6 in septin polymerization, perhaps stabilizing and facilitating filament growth through protein–protein interaction. Using Nanogold labeling during EM allowed an estimation of the stoichiometry of His-Orc6 binding to the septin filaments. We quantified the number of bound Nanogold particles (where each particle corresponds to one His-Orc6 molecule) per septin complex from EM images as shown in Figure 8. Assuming that each septin hexamer contains two Pnut molecules, and knowing that Orc6 interacts with Pnut, we expected to observe two Nanogold particles per monomer unit. The number of Nanogold particles associated with Orc6 molecules along the filaments was divided by the number of 24-nm septin hexamers composing the filaments. The experimental result was 2.26 ± 0.34 (n > 30 filaments were analyzed), which is very close to the expected 2:1 ratio.

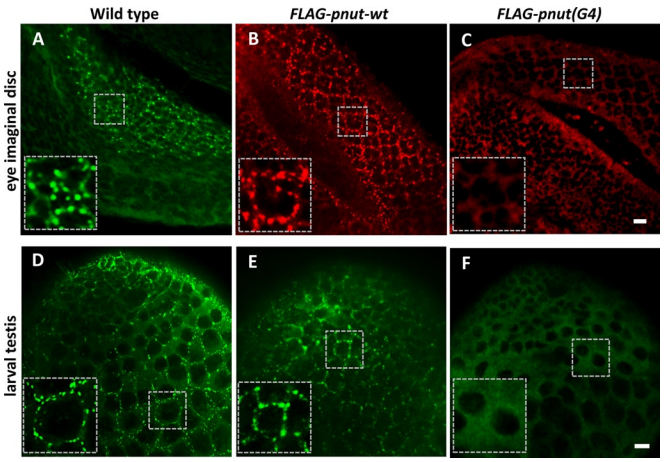

FIGURE 7: Mutations in GTPase domain disrupt Pnut membrane association. (A–C) Third-instar larvae eye imaginal disks. (D–F) Larval testes tips. Tissues presented are from wild-type (*Canton S*) flies (A, D) and fly strains carrying *pnut*^{XP} mutant rescued with wild-type *FLAG-pnut-wt* transgene (B, E) or *pnut*^{XP} mutant rescued with *FLAG-pnut (G4)* transgene (C, F). Anti-Pnut antibodies were used for immunostaining (green) in A and D–F, and anti-FLAG antibodies were used for immunostaining (red) in B and C. Scale bars, 10 μm.

Orc6 forms dimers in vitro and in vivo

We found that purified recombinant Orc6 protein behaves as a dimer in our biochemical assays. To test the ability of Orc6 to form dimers, we first purified the Orc6 protein to homogeneity and loaded it on a Superdex 75 sizing column (Figure 9A). The recombinant, highly purified Orc6 protein produces two peaks during separation on a Superdex 75 sizing column, corresponding to ~60 and 30 kDa. Silver-stained gel and Western blotting experiments (Figure 9A) confirmed the presence of Orc6 in both peaks, suggesting that the larger, ~60-kDa peak was formed by interaction of two Orc6 molecules. Full-length Orc6 protein often shows two close bands during PAGE due to partial degradation. Similar results were obtained when Orc6 Δ(200–257) mutant protein with deleted C-terminal domain (Figure 1A) was separated on a Superdex 75 column (Figure 9B), indicating that the observed dimerization of Orc6 does not require the C-terminal domain of the protein.

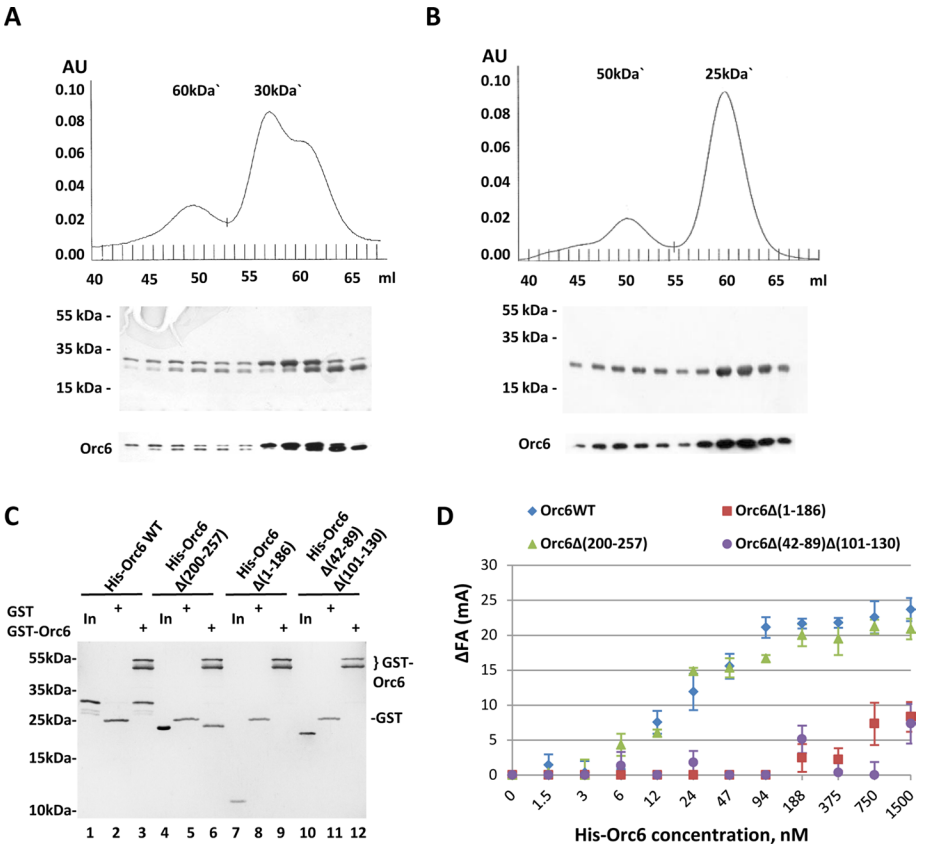

FIGURE 9: Orc6 protein forms dimers in vitro through the interaction of its N-terminal TFIIB-like domains. (A, B) Orc6 behaves as a dimer during purification on Superdex 75 sizing column. Separation profiles of (A) wild-type His-tagged Orc6 and (B) C-terminal deletion mutant His-Orc6 Δ(200–257). Silver-stained gel (~30 or ~25 kDa) and Western blot (-Orc6) of corresponding protein fractions are presented below each chromatography profile. (C) GST pull-down assay. His-tagged Orc6 wild type or mutant (In) was incubated with GST-Orc6-wt or GST (as a control), precipitated with glutathione beads, and analyzed with silver-stained SDS–PAGE. (D) Fluorescence anisotropy (FA) experiment: 130 nM GFP-tagged Orc6 WT was mixed with 1.5–1500 nM twofold serially diluted His-tagged Orc6 wild type or mutant in 50 µl of GTPase buffer. Three independent reactions were set up for each experiment. After 4 h of incubation, FA was measured, and ΔFA values were calculated by subtracting background (control reaction in the absence of His-tagged Orc6). Error bars, SD. Orc6 mutant abbreviations as in the legend to Figure 1.

To confirm these conclusions by a different technique and test the requirement of intact N-terminal TFIIB-like domain of Orc6 for dimerization, we analyzed the ability of wild-type and mutant Orc6 proteins to form dimers in pull-down experiments. Three types of Orc6 mutants (depicted in Figure 1A) were generated: Orc6 with deleted C-terminus, Orc6 Δ(200–257); Orc6 with deleted N-terminus, Orc6 Δ(1–186); and Orc6 with disrupted two globular N-terminal TFIIB-like domains, Orc6 Δ(42–89)Δ(101–130). His-tagged wild-type and mutant forms of Orc6 were incubated together with glutathione *S*-transferase (GST)–tagged wild-type Orc6 and precipitated in pull-down experiments using glutathione beads and wild-type GST-Orc6 as bait. The results are presented in Figure 9C. Wild-type Orc6 proteins and Orc6 Δ(200–257) mutant missing the C-terminal domain but containing the intact N-terminal domain can be precipitated together, as seen by the presence of both GST- and His-tagged versions of the protein in the pull- down material (lanes 3 and 6, respectively). However, Orc6 mutants with deleted or disrupted N-terminal TFIIB-like domain were not detected in pull-down material precipitated by glutathione beads together with GST-tagged wild type Orc6 (lanes 9 and 12), suggesting the importance of the TFIIB-like domain for Orc6–Orc6 interaction.

Next we performed equilibrium binding experiments using fluorescence anisotropy and GFP-labeled Orc6. In these kinds of experiments, if the fluorophore-bound protein binds another protein, the rotational rate decreases, resulting in an increase of anisotropy. As shown in Figure 9D, full-length GFP-Orc6 bound to the wild-type His-tagged Orc6 protein (blue diamonds). Consistent with the pull-down results, the Orc6 Δ(200–257) mutant with deleted C-terminus (green triangles) bound to wild-type GFP-tagged Orc6 with the same affinity as the full-length protein. In contrast, the C-terminal 71 amino acid residues of Orc6 missing the N-terminal domain (red squares) or mutant with disrupted N-terminal domain (purple circles) failed to interact with GFP-tagged wild-type Orc6 protein (Figure 9D). Together these results show that structurally conserved N-terminal domain of *Drosophila* Orc6 is important for dimerization of Orc6 protein.

To examine whether Orc6 protein can form dimers in vivo, we performed fluorescence resonance energy transfer (FRET) experiments. In these experiments, efficient FRET can be detected only if two proteins exist in close proximity to each other, often forming a complex. We coexpressed cyan fluorescent protein (CFP)– and yellow fluorescent protein (YFP)–tagged Orc6 proteins together in *Drosophila* S2 tissue culture cells. Cells expressing both CFP-Orc6 and YFP-Orc6 were fixed and analyzed with acceptor photobleaching FRET. The results are presented in Figure 10. We compared the obtained FRET efficiencies using a positive control FRET construct consisting of a CFP-YFP fusion protein. Negative control consists of CFP and YFP proteins coexpressed separately in the cells. FRET results for CFP- and YFP-tagged coexpressed Orc6 proteins are presented for the nucleus, cytoplasm, and membranes. The highest FRET efficiency for coexpressed CFP- and YFP-tagged Orc6 molecules was detected at the cell membranes (Figure 10A; representative experimental cells are presented in Figure 10B), which is consistent with Orc6 and Pnut colocalization in *Drosophila* cells and tissues (Chesnokov *et al.*, 2001, 2003; Huijbregts *et al.*, 2009). No positive FRET was detected in the cytoplasm or in the nucleus of tissue culture cells (Figure 10, A and B). Orc6 mutants with deleted C-terminal domain were unable to interact with Pnut and failed to localize to the membranes, as we described earlier (Chesnokov *et al.*, 2003).

Orc6–Orc6 interaction is important for septin filament formation facilitated by Orc6

Next we tested septin complex filament formation in the presence of wild-type Orc6, as well as Orc6 mutant proteins (Figure 1B). The results are shown in Figure 11. Wild-type Orc6 protein stimulated filament formation (Figure 11A) but Orc6 mutants

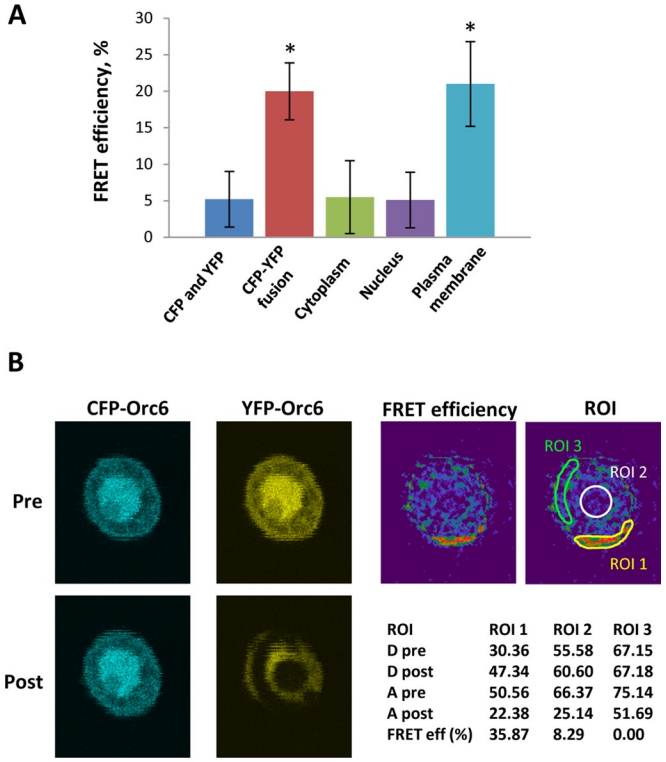

ROI	ROI 1	ROI 2	ROI 3
D pre	30.36	55.58	67.15
D post	47.34	60.60	67.18
A pre	50.56	66.37	75.14
A post	22.38	25.14	51.69
FRET eff (%)	35.87	8.29	0.00

FIGURE 10: Orc6 forms homodimers in vivo. (A) S2 cells expressing CFP-Orc6 and YFP-Orc6 were fixed and analyzed with acceptor photobleaching FRET. FRET efficiencies for cytoplasm, nucleus, and plasma membrane regions are shown (minimum five cells were examined). Error bars, SD. Negative control corresponds to CFP and YFP proteins expressed separately in cells. Positive FRET corresponding to $FRET_{eff}$ for CFP-YFP fusion is also presented. Asterisks indicate significant difference relative to the negative control (Student's *t* test, $p < 0.05$). (B) Representative experiment. FRET efficiency is depicted in color: blue is low efficiency, red is high efficiency. pre, prebleach image; post, postbleach image; D, donor (CFP-Orc6); A, acceptor (YFP-Orc6); ROI, region of interest; ROI1, cell membrane; ROI2, nucleus; ROI3, cytoplasm.

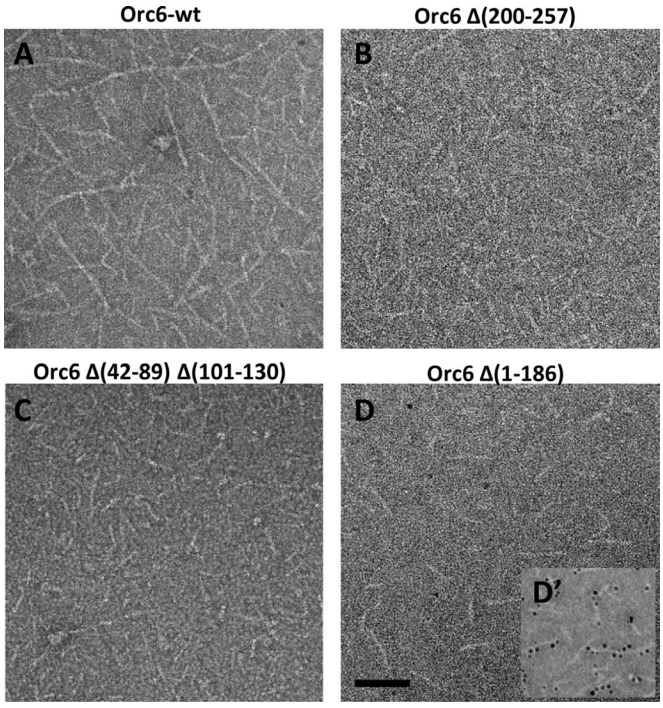

FIGURE 11: Orc6 dimerization is important for septin filament formation facilitated by Orc6. Recombinant wild-type septin complex (10 ng/μl) was incubated with Orc6 (15 ng/μl) wild type or mutant and then visualized by negative-stain transmission EM. (A) Orc6-wt; (B) Orc6 Δ(200–257), mutant missing C-terminal domain; (C) Orc6 Δ(42–89)Δ(101–130), mutant missing parts of two globular TFIIB-like domains; (D) Orc6 Δ(1–186), mutant missing N-terminal domain. (D′) For Orc6Δ (1–186), association with septin complex was shown using gold labeling as in Figure 8. Scale bar, 100 nm.

missing parts of or the entire TFIIB-like domain did not (Figure 11, C and D). Orc6 Δ(200–257) mutant missing C-terminal domain is unable to interact with Pnut and therefore was unable to facilitate septin filament formation, as shown earlier (Huijbregts *et al.*, 2009) and in Figure 11B. The C-terminal domain of Orc6 alone, Orc6 Δ(1–186), was able to interact with Pnut and septin complex (Huijbregts *et al.*, 2009; this study); however, it was not sufficient to stimulate polymerization, as shown in Figure 11D. As shown in the inset in Figure 11D′, even though His-tagged C-terminal Orc6 fragment localized at the short septin complex fragments under EM conditions as shown by Nanogold staining, these fragments failed to polymerize and organize into larger filaments. To test the hypothesis that dimerization by itself could drive septin polymerization, we substituted the N-terminal TFIIB-like domain of Orc6 with GST, known to form homodimers (McTigue *et al.*, 1995). In particular, we tested two different recombinant proteins—one with GST directly fused to the C-terminal domain of Orc6 (Orc6 Δ(1–186)) and another containing a linker of three Gly residues between GST and Orc6 Δ(1–186), which could provide more flexibility between two parts. As shown in Supplemental Figure S6, neither of the GST-tagged proteins (~35 kDa) stimulated septin filament formation at the same concentration as wild-type Orc6 (~33 kDa). Instead, we observed multiple aggregates lying between septin rods, which may represent GST-Orc6 Δ(1–186) homodimers or aggregates. At higher concentrations of GST-tripleGly-Orc6 Δ(1–186), we did observe some filament formation (Supplemental Figure S6), suggesting that dimerization of Pnut-interacting proteins may in some cases facilitate septin polymerization. Taken together, these data suggest that N-terminal TFIIB-like domain and C-terminal domain of Orc6 are both involved in septin filament formation. In summary, we conclude that Orc6 protein plays an important role in septin polymerization. This function of the protein is correlated with its ability to form dimers both in vitro and in vivo.

DISCUSSION

A number of open questions remain with regard to the septins, such as the mechanisms of septin polymer assembly and disassembly in different organisms and how GTP binding and hydrolysis might be coupled to changes in the structure and activity of the proteins. Although GTP binding renders septin complexes competent for polymerization (Field *et al.*, 1996; Mendoza *et al.*, 2002; Versele and Thorner, 2004; Sirajuddin *et al.*, 2009), additional factors, such as posttranslational modifications (Johnson and Blobel, 1999; Zhang *et al.*, 2000; Dobbelaere *et al.*, 2003) and interacting partners (Joberty *et al.*, 2001; Kinoshita *et al.*, 2002; Nagata *et al.*, 2003; Bertin *et al.*, 2010), appear to regulate the dynamics of septin filament formation and breakdown in cells. Regulation of the size of septin filaments is essential during the whole cell cycle, as both higher-order septin assemblies, such as septin rings at the

cleavage furrows, as well as smaller, dispersed septin scaffolds, have been found (Kinoshita, 2006). Our earlier studies identified Orc6 protein, which may be directly involved in this process (Huijbregts *et al.*, 2009).

Septins interact to form larger complexes. The best-characterized septin complex is isolated from budding yeast and comprises four septins found in equal amounts (Haarer and Pringle, 1987; Ford and Pringle, 1991; Kim *et al.*, 1991). The basic structural unit of the yeast septin complex is an octamer, composed of four subunits, organized into two tetramers with twofold rotational symmetry (Bertin *et al.*, 2008). The structure of human heterotrimeric (SEPT2-SEPT6-SEPT7) septin complex was also solved (Sirajuddin *et al.*, 2007). Similar to yeast octamer, the human complex structure is an apolar hexamer with each septin arranged symmetrically. Recent data indicate that mammalian septin hexamer may in some cases also include SEPT9 protein, resulting in the formation of an octamer, as in yeast (Kim *et al.*, 2011, 2012; Sellin *et al.*, 2011, 2012). No data indicate that *Drosophila* septin complex forms an octamer. Highly purified native *Drosophila* complex consists of Pnut, Sep1, and Sep2 subunits (Field *et al.*, 1996; Huijbregts *et al.*, 2009). The analysis of immunoprecipitated material from *Drosophila* tissue and cell extracts revealed the presence of the same three septins (Field *et al.*, 1996; Huijbregts *et al.*, 2009). On the basis of the sequence homologies between human and *Drosophila* septins (Pan *et al.*, 2007), we proposed that *Drosophila* septin complex might be arranged in a similar way, which would put Pnut protein at either end of the complex (Huijbregts *et al.*, 2009). The human SEPT2-SEPT6-SEPT7 complex can be formed from recombinant proteins all lacking their predicted coiled-coil domains (Sirajuddin *et al.*, 2007). In fact, structural analysis of human septin complex revealed that the hexamers consist of an assembly of GTP-binding domains. However, the coiled-coil domains of SEPT6 and SEPT7 do interact directly with each other (Low and Macara, 2006), suggesting that, although not required for the formation of human septin complex, coiled-coils may further stabilize septin polymerization (Sirajuddin *et al.*, 2007). The GTP-binding domains of human septin proteins can also interact with coiled-coil structures within the multiple subunit complex (Low and Macara, 2006). This might even be more important for *Drosophila* septins when they assemble into the complex. We found that the deletions of Pnut CTD or CTD of all septins constituting the *Drosophil*a septin complex (Pnut, Sep1, and Sep2) result in the inability of *Drosophila* septins to form a complex (Huijbregts *et al.*, 2009; this study). Moreover, the interaction of Orc6 with the septin complex and the stimulating effect of Orc6 on septin complex activities seem strongly dependent on the coiled-coil domain of Pnut (Huijbregts *et al.*, 2009).

Our in vivo data reported in this study confirm the importance of CTD in Pnut for septin complex formation. Pnut transgene missing the C-terminal domain is unable to rescue the lethal *pnut* null-allele phenotype. Cytological analysis shows that the coiled-coil domain of Pnut, which is important for *Drosophila* septin complex assembly, is also essential for the in vivo localization of Pnut, as FLAG-Pnut(1–427), lacking this domain, had the tendency to accumulate into aggregates (Figure 5). Similar aggregates were observed when Pnut lacking CTD was expressed in *Drosophila* tissue culture L2 cells (Huijbregts *et al.*, 2009). Of interest, cells containing Pnut with deleted CTD showed mislocalization of other septins comprising the septin complex in *Drosophila* (Figure 5), indicating the importance of this motif for septin complex localization in vivo. In the absence of Pnut due to RNAi, membrane localization of other members of the *Drosophila* septin complex was also lost, as shown in Supplemental Figure S5 for Sep1 protein. The loss of Sep1 localization was previously reported in Pnut-deficient *Drosophila* embryos (Adam *et al.*, 2000). It was proposed that different septin complexes may form within *Drosophila* during development (Adam *et al.*, 2000). Of interest, Pnut G4 mutant did not rescue null-allele flies; however, no visible cytokinetic defects were observed in neural ganglia or imaginal disks of mutant larvae. Immunofluorescence experiments using anti-Pnut and anti-FLAG antibodies showed that FLAG-Pnut G4 mutant protein did not display characteristic intense, dot-like staining at the membranes in imaginal disks and testes. Instead, diffuse staining was detected in the membrane region. It might be that even though PnutG4 mutant was still associated with membranes, the resulting septin complex could not form specific structures, most probably because of its compromised ability to form filaments (Figure 4). The other possibility is that maternally contributed wild-type Pnut, together with mutant Pnut G4, could form partially functional heterogeneous septin complexes and filaments, which allow further developmental progression. Perhaps Pnut G4 mutant may partially rescue cytokinesis defects but not other developmental or tissue building processes in which Pnut normally participates. For example, Pnut showed a high level of expression in the nervous system, and *pnut* was originally discovered as a gene involved in photoreceptor development (Neufeld and Rubin, 1994). Pnut is also important for adherent junction remodeling in epithelial cells (Founounou *et al.*, 2013).

All septins contain a central Ras-like domain that binds GTP, and most septins hydrolyze it to GDP (Leipe *et al.*, 2002; Pan *et al.*, 2007). Structural studies of human septin subgroups carried out during recent years suggest that septins interact with each other using two distinct interfaces, one composed of the nucleotide-binding site, called the G interface, and the other involving the amino and carboxyl termini, called the NC interface (Sirajuddin *et al.*, 2007, 2009; Zent *et al.*, 2011; Wittinghofer and Zent, 2014). GTP hydrolysis appears to induce stable conformational changes in the septin–septin interaction interfaces. For example, GTP binding by SEPT2 (human homologue of *Drosophila* Sep1) induces conformational change in the G interface, which is transmitted to the NC interface (Sirajuddin *et al.*, 2009). SEPT7 (human homologue of *Drosophila* Pnut) forms a tight G-interface dimer in a GDP-bound state (Wittinghofer and Zent, 2014). SEPT6 (Sep2 in *Drosophila*), on the other hand, does not possess any GTPase activity and is found in a complex with other septins in GTP-bound form (Sirajuddin *et al.*, 2007). A structural rather than regulatory role for septin complex–bound GTP and GDP was proposed from the results obtained with yeast septins (Vrabioiu *et al.*, 2004). No turnover of yeast septin-bound GTP and GDP could be detected during a cell cycle in vivo. Furthermore, in vitro experiments revealed that GTP hydrolysis of yeast septin complex was limited by its slow binding or exchange activity, similar to the properties described initially for the *Drosophila* septin complex (Field *et al.*, 1996).

In our studies, we found that mutations in all three GTPase motifs (G1, G3, and G4) of Sep2 and Sep1 result in disassembly of the septin complex, supporting the structural role of GTP and Sep2 in the formation of heterotrimeric complex as Sep2 interacts with Sep1 through the G interface, as suggested by structural studies of the human septin complex (Sirajuddin *et al.*, 2007). Pnut and Sep1 GTPase single mutants were able to reconstitute into soluble septin complex but displayed significant defects in filament formation. On the basis of published studies (Sirajuddin *et al.*, 2007, 2009; Zent *et al.*, 2011; Wittinghofer and Zent, 2014) and our results, one could imagine that Sep1 GTPase mutants affected the stability of the NC interface between two septin trimers, resulting in their inability to form functional hexameric complex and further assemble into

filaments (as shown in Figure 4). GTPase mutations in Pnut (localized on the either end of septin hexamer), on the other hand, might disrupt tight interaction between G domains and result in a failure of septin hexamers to polymerize. It appears that nucleotide-dependent changes in septin structure that facilitate or block septin–septin interactions may be a common theme in septins that cycle between GTP and GDP.

Orc6 protein is the least conserved and probably the most enigmatic among ORC subunits. It is important for DNA replication in all species (Dutta and Bell, 1997). In both *Drosophila* (Chesnokov *et al.*, 2001) and human cells (Prasanth *et al.*, 2002), a considerable pool of Orc6 is cytoplasmic, and the protein is either associated with or proximal to the plasma membrane and cleavage furrows of dividing cells. In *Drosophila*, Orc6 and Pnut colocalize in vivo at cell membranes and cleavage furrows of dividing cells and during cellularization in *Drosophila* early embryos (Chesnokov *et al.*, 2003). The C-terminal domain of Orc6 is required for the interaction with Orc3 during formation of the six-subunit ORC complex and with Pnut; however, these interactions are mediated by different motifs within C-terminal domain of Orc6 (Chesnokov *et al.*, 2003; Huijbregts *et al.*, 2009; Bleichert *et al.*, 2013). The C-terminus of Orc6 is also necessary for colocalization with Pnut in *Drosophila* cells and tissues (Chesnokov *et al.*, 2003). Moreover, Orc6 RNAi results in cytokinesis defects in *Drosophila* tissue culture cells (Chesnokov *et al.*, 2003), and Pnut RNAi disrupts the localization of Orc6 to the plasma membrane (Huijbregts *et al.*, 2009).

We previously found that Orc6 facilitates GTPase activity and filament formation of septin complex in *Drosophila* (Huijbregts *et al.*, 2009). In this study, we concentrated on the mechanism of Orc6's role in regulating septin complex activities. We found that increasing the concentration of GTP toward saturation in the presence of Orc6 did not result in filament disassembly but further stimulated septin polymerization (Figure 3). Note that our earlier experiments (Huijbregts *et al.*, 2009) were performed in the presence of low concentrations of GTP. In this study, to avoid the potential problem of depleting GTP in reactions, we used a range of higher concentrations of nucleotides. Under these conditions, the addition of Orc6 allows efficient polymerization of septin complex at concentrations of protein significantly less than those necessary for polymerization in solution.

The role of Orc6 in septin complex polymerization is summarized in the model presented in Figure 12. Orc6 molecules interact with each other and therefore are able to facilitate septin complex filament formation by bringing together two Pnut molecules of two adjacent septin hexamers. Nanogold staining allowed direct visualization and quantification of Orc6 molecules on septin filaments (two molecules of Orc6 per septin hexamer). This localization of Orc6 depends on the amphipathic α-helical domain of the Orc6 located in the C-terminus of the protein. The C-terminal domain of Orc6 binds the coiled-coil domain of Pnut, which is positioned at the either end of septin hexamer. Orc6 then dimerizes and facilitates GTP-to-GDP hydrolysis by Pnut, resulting in tighter G-domain interactions between GDP-bound Pnut molecules of two adjacent septin hexamers. Recent data for human septins indicate that SEPT7 (Pnut in *Drosophila*) forms very tight G interface dimers in a GDP-bound state (Zent *et al.*, 2011; Wittinghofer and Zent, 2014). Orc6–Orc6 interactions further stabilize septin filaments. In support of this model, we found that Orc6 forms dimers both in vitro and in vivo. During size exclusion chromatography, the protein forms two peaks corresponding to ~30 and ~60 kDa. Orc6 dimerization was also confirmed in our pull-down assays. As shown by mutational analysis, the ability of Orc6 to form dimers depends on an intact N-terminal

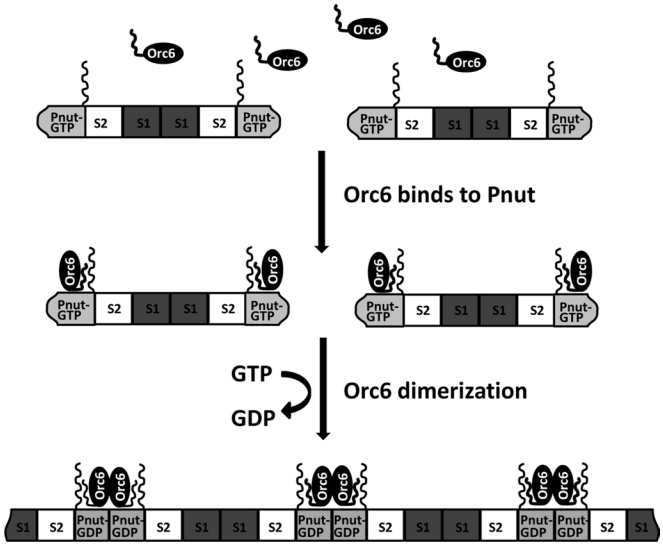

FIGURE 12: Model. See the text for details.

TFIIB-like domain of the protein, which is also required to stimulate septin polymerization. Furthermore, Orc6 forms dimers in vivo, as documented by FRET experiments. Of importance, the highest FRET efficiency for coexpressed CFP- and YFP-tagged Orc6 proteins was observed at the membranes (Figure 10), where Orc6 colocalized with Pnut (Chesnokov *et al.*, 2003). We previously showed that ablation of Pnut in tissue culture cells during RNAi experiments results in loss of membrane association for Orc6 (Huijbregts *et al.*, 2009). The expression of Orc6 mutants unable to interact with Pnut also resulted in cytokinesis defects in *Drosophila* tissue culture cells (Chesnokov *et al.*, 2003). Taken together, our data strongly suggest direct involvement of Orc6 in septin polymerization.

It would be interesting to analyze whether Orc6 may also form dimers on DNA in the nucleus of actively replicating and dividing cells. We previously showed that Orc6 binds DNA and may participate in positioning of the entire ORC complex at the origins during formation of the prereplicative complex. Orc6–Orc6 interactions then would potentially help in the assembly of two ORC complexes together at the origins during G1 phase of the cell cycle, allowing mini-chromosome maintenance (MCM) proteins loading in both directions. We did detect elevated FRET efficiency in some of the cells in the nucleus compared with cytoplasm during our FRET experiments; however, a conclusive experiment would require careful FRET analysis at different stages of the cell cycle using synchronized tissue culture cells.

The septins are important for cytokinesis, but the molecular mechanisms of their functions in this process are not completely understood. The active role for Orc6 in regulating septin complex functions suggests that it may couple DNA replication and cytokinesis pathways and/or assist in a targeting function for septins in metazoans, potentially linking the completion of DNA replication and the assembly of septin rings at the cleavage furrow. Our data also represent a functional dissection of *Drosophila* septins and reveal new aspects of these proteins, highlighting basic conserved and divergent features among metazoan septin complexes.

MATERIALS AND METHODS

Cloning and mutagenesis

Available cDNAs of Pnut, Sep2, and Sep1 (*Drosophila* embryonic MATCHMAKER library; Clontech Laboratories, Mountain View, CA)

were used to generate mutations in the GTPase domain and deletion mutants. Isolation of Orc6 cDNA has been described (Chesnokov *et al.*, 1999). Amino acid substitutions were introduced with site-directed mutagenesis (www.chem.agilent.com/Library/usermanuals/Public/200518.pdf). Substitutions generated were Pnut(K155A), Pnut(D206A), Pnut(K288A), Pnut(K155A,D206A,K288A), Sep1(K48A), Sep1(D99A), Sep1(K181A), Sep1(K48A,D99A,K181A), Sep2(K56A), Sep2(D102A), Sep2(K186A), and Sep2(K56A,D102A,K186A). Septin C-terminal deletions Pnut(1–460), Pnut(1–427), Sep1(1–328), and Sep2(1–336) and Orc6 deletion mutants Orc6 Δ(200–257), Orc6 Δ(1–186) and Orc6 Δ(42–89)Δ(101–130) were generated with standard PCR techniques using appropriate primers to remove desired domains. All constructs were analyzed by sequencing. cDNAs encoding wild-type and mutant proteins were subcloned into desired vectors with standard molecular biological techniques.

Proteins and antibodies

cDNAs coding for wild-type, GTPase, and C-terminal deletion mutants of Pnut and Sep1 were cloned into the pET-Duet expression vector to generate N-terminal His-tagged proteins. cDNAs coding for wild-type, GTPase, and C-terminal deletion mutants of Sep2 were cloned into the pGEX-4T1 expression vector to generate GST-tagged proteins. Plasmids were transformed into *E. coli* strain BL21 DE3. Colonies were grown in Miller's LB Broth with 100 μg/ml ampicillin at 37°C to an OD_{600} of 0.6. Cultures were transferred to 16°C, and protein expression was induced with 0.4 mM isopropyl-β-D-thiogalactoside (IPTG) overnight. Cells were lysed in a French press, after which His-Sep1 and His-Pnut proteins were isolated with HisPur Cobalt resin (Thermo Scientific, Rockford, IL), and GST-Sep2 was recovered using Pierce glutathione agarose (Thermo Scientific) according to the manufacturer's recommendations. Pnut proteins were further purified on a 5-ml HP SP column (GE Healthcare, Uppsala, Sweden). Protein was eluted from the column using a gradient of 100 mM–1 M NaCl in 25 mM 4-(2-hydroxyethyl)-1-piperazineethanesulfonic acid (HEPES)–NaOH, pH 8.0, 2 mM $MgCl_2$, 0.1 mM EDTA, 5% glycerol, and 1 mM dithiothreitol (DTT). Sep1 and Sep2 proteins were further purified on a 5-ml HP Q column (GE Healthcare). Proteins were eluted from the column using a gradient of either 50 mM for Sep1 or 100 mM for Sep2 to 1 M NaCl in 25 mM HEPES-NaOH, pH 8.0, 2 mM $MgCl_2$, 0.1 mM EDTA, 5% glycerol, and 1 mM DTT. The GST tag was removed from GST-Sep2 protein using thrombin protease.

Purified His-Sep1 and Sep2 antigens were used to generate rabbit polyclonal antibodies (Cocalico Biologicals, Reamstown, PA). Antibodies were purified by affinity chromatography as described previously (Huijbregts *et al.*, 2009).

Recombinant baculoviruses were generated and septin complexes reconstituted as described previously (Huijbregts *et al.*, 2009). Eluate fractions containing septin complex His-Pnut-Sep2-Sep1 were diluted to 50 mM NaCl and further purified with anion chromatography on a 1-ml HiTrap HP Q column using a gradient of 50 mM–1 M NaCl in 25 mM HEPES, pH 8.0, 2 mM $MgCl_2$, 0.1 mM EDTA, 5% glycerol, and 1 mM DTT. The septin complex eluted at ~200 mM NaCl.

Wild-type or mutant Orc6 cDNAs were cloned into pQE-30 or pGEX-4T1 expression vectors generating N-terminal His- or GST-tagged Orc6, respectively. For the GFP-Orc6 construct, wild-type Orc6 cDNA was fused with wild-type GFP and subcloned into pQE-30 expression vector, generating N-terminal His-GFP-Orc6. Plasmids were transformed into *E. coli* strain M15. Colonies were grown in Miller's LB Broth with 100 μg/ml ampicillin and 25 μg/ml kanamycin at 37°C to an OD_{600} of 0.6, and protein expression was induced with 1 mM IPTG for 4 h. Cells were collected and disrupted in a French press. His-Orc6 or GST-Orc6 was isolated using HisPur Cobalt resin or Pierce glutathione agarose, respectively. His-Orc6 or GST-Orc6 proteins were further purified on a 5-ml HP SP column using a gradient of 100 mM–1 M NaCl in 25 mM HEPES, pH 7.6, 2 mM $MgCl_2$, and 1 mM DTT. Protein fractions containing His-Orc6 or GST-Orc6 were further separated on Superdex 75 10/300 GL (GE Healthcare) sizing column in 25 mM HEPES, pH 7.6, 2 mM $MgCl_2$, 100 mM NaCl, and 1 mM DTT. Wild-type His-GFP-Orc6 was purified on Superdex 75 10/300 GL in 25 mM HEPES, pH 7.6, 2 mM $MgCl_2$, 300 mM NaCl, and 1 mM DTT.

HiLoad Superdex 75 16/600 (GE Healthcare) was used for separation of monomeric and dimeric forms of Orc6. Buffer used was 25 mM HEPES, pH 7.6, 2 mM $MgCl_2$, 100 mM NaCl, and 1 mM DTT.

GTPase assays

GTP assays for individual septins. A 50-μg amount of His-Pnut or His-Sep1 protein or 100 μg of Sep2 protein was diluted in a total volume of 200 μl of GTPase buffer (25 mM HEPES-KOH, pH 7.6, 2 mM $MgCl_2$, 1 mM ethylene glycol tetraacetic acid [EGTA], 50 mM KCl, 1 mM DTT) containing 5 μCi of [α-^{32}P]GTP (3000 Ci/mmol; GE Healthcare) and cold GTP at a concentration of 2 μM. Reactions were incubated at 21°C for 4 h. Aliquots of 100 μl were diluted with 900 μl of ice-cold GTPase buffer and applied to 25-mm nitrocellulose membrane filters (0.22 μm; EMD Millipore, Billerica, MA) connected to a vacuum manifold (EMD Millipore). The filters were washed six times with 3 ml of ice-cold GTPase buffer. Incorporation of GTP into septin protein was analyzed by measuring ^{32}P radioactivity on the filters with liquid scintillation counting. GTP hydrolysis was analyzed by eluting nucleotides bound to the septin on the filter with 100 μl of 8 M urea, 5 mM EDTA, and 20 mM Tris-HCl, pH 7.5. A 10-μl amount of the eluate was analyzed for nucleotides by TLC on polyetheleneimine-cellulose plates (Selecto Scientific, Suwanee, GA). Urea was removed by developing the plates in water. Plates were air dried and then developed with 0.85 M KH_2PO_4, pH 3.4. Radioactive GTP and GDP spots were quantified by phosphorimaging.

GTP binding of recombinant septin complexes. A 2-μg amount of recombinant septin complex His-Pnut-Sep2-Sep1 (wild type or mutant) was diluted in 25 μl of GTPase buffer (with the addition of 0.05 mg/ml bovine serum albumin) containing 5 μCi of [α-^{32}P]GTP (3000 Ci/mmol; GE Healthcare) and 2 μM cold GTP and incubated at 21°C for 1 h. Then the reaction was diluted 10-fold with GTPase buffer, and five aliquots of 50 μl were filtered through a 0.22-μm nitrocellulose membrane using a vacuum manifold (Bio-Dot SF; Bio-Rad, Hercules, CA). The membrane in each well was washed four times with 1 ml of GTPase buffer, air dried, and counted in a liquid scintillation counter.

GTP hydrolysis of recombinant septin complexes. A 4-μg amount of recombinant septin complex (wild type or mutant) was diluted in 20 μl of GTPase buffer with the addition of phosphate sensor (Invitrogen, Carlsbad, CA) to a concentration of 2 μM. The reaction was started with the addition of GTP to a concentration of 100 μM. Phosphate sensor is a phosphate-binding protein modified with a fluorophore. As the sensor binds free P_i, fluorescence intensity increases. The measurement was taken with a Synergy 2 multimode microplate reader (Biotek, Winooski, VT) at excitation of 360(40) nm and emission of 460(40) nm.

Electron microscopy

Recombinant baculovirus-derived wild-type or mutant septin complex His-Pnut-Sep2-Sep1 was diluted in GTPase buffer (25 mM HEPES-KOH, pH 7.6, 2 mM $MgCl_2$, 1 mM EGTA, 50 mM KCl) to 10 ng/µl. Where indicated, 15 ng/µl His-Orc6 wild type or mutant and GTP, GDP, or GTPγS were added to the reaction. Samples were incubated at 22°C for 2 h, after which they were applied to copper Formvar carbon-coated grids and incubated at room temperature for 3 min. Excess solution was removed from the grids, and proteins were fixed with 1% uranyl acetate in 30% ethanol for 1 min. Fixative was removed and grids dried, after which images were taken on a FEI Tecnai F20 electron microscope operated at 200 kV.

Frequencies of monomer–*n*-mer filaments were quantified from 10 EM images (>800 filaments) for each reaction of filament formation (no nucleotide, with 1 mM GTP, 1 mM GDP, or 1 mM GTPγS) and grouped based on the length. We considered 24 nm as the length of a monomer septin complex (Field *et al.*, 1996; Mavrakis *et al.*, 2014). A chi-square test was performed, where expected frequencies for the reactions with GTP, GDP, or GTPγS were calculated from the distribution of frequencies in the control experiment (without any nucleotide). Standardized residuals were quantified for each group as (observed count − expected count)/√(expected count). Groups in which standardized residual values were greater than 2 considered to contribute most to the difference between two distributions.

To localize His-tagged Orc6 on septin filaments, His-tag was removed from wild-type septin complex His-Pnut-Sep2-Sep1 using AcTEV protease according to the manufacturer's protocol (Invitrogen). His-Orc6 (15 ng/µl) was incubated with wild-type septin complex Pnut-Sep2-Sep1 (20 ng/µl) in the presence or absence of 1 mM GTP as described. Samples were applied on EM grids, and His-Orc6 was labeled with 5 nm Ni-NTA Nanogold following the manufacturer's protocol (2082; Nanoprobes, Yaphank, NY). EM images from three independent labeling experiments (>30 filaments) were analyzed to determine the stoichiometry of His-Orc6 binding to the septin monomer complex. For that, the number of Nanogold particles (where each particle corresponds to one His-Orc6 molecule) labeling each filament was divided by the number of 24-nm monomers composing the filament.

Fly stocks

All crosses were carried out at 25°C under standard conditions. cDNAs of wild-type Pnut-wt, Pnut(K288A), Pnut(K155A,D206A,K288A), and C-terminal deletion Pnut(1–427) were inserted into pCasper3 under the 1.7-kb native Pnut promoter, followed by FLAG. All constructs were injected into w^{1118} *Drosophila* embryos, and individual transgenic strains were set up. Expression of transgenic proteins was verified by Western blots. For rescue experiments, heterozygous females and males of genotype w^{1118}; $pnut^{XP}$/Cy; FLAG-pnut-wt/+, w^{1118}; $pnut^{XP}$/Cy; FLAG-pnut(K288A)/+, w^{1118}; $pnut^{XP}$/Cy; FLAG-pnut(K155A,D206A,K288A)/+, or w^{1118}; $pnut^{XP}$/Cy; FLAG- pnut(1-427)/+, where $pnut^{XP}$ is a molecular null allele (Neufeld and Rubin, 1994), were crossed, and the percentage of rescued flies was calculated based on expected segregation. *Canton-S* was used as a standard strain for immunostaining.

Cytology

Preparation of mitoses was described previously (Lebedeva *et al.*, 2000). Briefly, third-instar larval neural ganglia were incubated in 0.075 M KCl for 5 min, fixed in methanol with acetic acid (3:1) for 20 min, and then dispersed in a drop of 50% propionic acid on a slide. Then slides were dried and stained with 5% Giemsa's solution.

Imaginal disks and testes of third-instar larvae were dissected in Ephrussi-Beadle Ringer solution (7.5 g of NaCl, 0.35 g of KCl, and 0.279 g of $CaCl_2{\cdot}2H_2O$ in 1 l of distilled water) and fixed in 4% formaldehyde in phosphate-buffered saline (PBS) for 20 min, washed twice for 15 min in PBS containing 0.3% Triton X-100 (PBT), and blocked for 1 h with 10% goat serum in PBT. Samples were then incubated overnight at 4°C with any of the following primary antibodies diluted in PBT containing 10% goat serum: rabbit anti-Pnut (1:1000; Huijbregts *et al.*, 2009), mouse anti-Pnut (4C9H4: G. M. Rubin, Developmental Studies Hybridoma Bank, Iowa City, IA; 1:500), rabbit anti-Sep1 (1:1000), rabbit anti-Sep2 (1:1000), mouse anti–α-spectrin (3A9: D. Branton and R. Dubreuil, Developmental Studies Hybridoma Bank; 1:30), mouse anti-FLAG (Sigma-Aldrich, St. Louis, MO; 1:500). These primary antibodies were detected by 2-h incubation at room temperature with secondary antibodies conjugated to Alexa 488 or Alexa 568 (Molecular Probes, Eugene, OR; 1:1000). Nuclei were counterstained with 4′,6-diamidino-2-phenylindole (Roche Diagnostics GmbH, Mannheim, Germany), and slides were mounted with 80% glycerol, 20% 1× PBS, and 2% *N*-propyl gallate. Images were taken with an Olympus BX61 motorized upright microscope fitted with a BX-DSU disk scan unit.

GST pull-down assay

A 100-pmol amount of wild-type or mutant His-tagged Orc6 was incubated with 20 pmol of GST or GST-Orc6 wild type for 2 h in pull-down buffer (25 mM HEPES, pH 7.6, 50 mM KCl, 2 mM $MgCl_2$, 1 mM EDTA, 10% glycerol, 0.01% Triton X-100) in the presence of 0.1% casein (70955; Novagene, Madison, WI). Then 2.5 µl of Pierce glutathione agarose was added to the reaction and incubated for 30 min, after which beads were washed three times with pull-down buffer. Bound proteins were dissociated from beads by boiling in SDS–PAGE loading buffer and analyzed by gel electrophoresis, followed by silver staining.

Fluorescence polarization assay

GFP-tagged wild-type Orc6, 130 nM, was mixed with 1.5–1500 nM twofold serially diluted His-tagged Orc6 wild type or mutant in 50 µl of GTPase buffer (25 mM HEPES-KOH, pH 7.6, 2 mM $MgCl_2$, 1 mM EGTA, 50 mM KCl). Three independent reactions were set up for each experiment. After 4 h of incubation, fluorescence anisotropy (FA) was measured on a Synergy 2 multimode microplate reader at excitation 485(20) nm and emission 528(20) nm. ΔFA values were calculated by subtracting background (control reaction in the absence of His-tagged Orc6).

FRET analysis

Drosophila S2 cells were grown in M3 medium (Sigma-Aldrich) and cotransfected with pMT-CFP-Orc6 and pMT-YFP-Orc6. Construct pMT-CFP-YFP was used as a positive control; pMT-CFP and pMT-YFP were expressed separately for a negative control. Transfection was performed using Cellfectin reagent (Invitrogen) according to the manufacturer's protocol. After overnight incubation, expression was induced by the addition of 0.5 mM $CuSO_4$ for 24 h, after which cells were fixed in 2% formaldehyde in PBS for 10 min. FRET was measured using the acceptor photobleaching method (Karpova and McNally, 2006). According to this procedure, if FRET is occurring, then photobleaching of the acceptor (YFP) should yield a significant increase in fluorescence of the donor (CFP). Data were acquired and analyzed using a Leica DMRB SP2 confocal microscope with default CFP/YFP settings. FRET efficiency was calculated as $FRET_{eff} = (D_{post} - D_{pre})/D_{post}$ for all $D_{post} > D_{pre}$, where D is donor. For our protocol, we considered $FRET_{eff} \geq 20\%$ as positive FRET (corresponding to

$FRET_{eff}$ for positive control with pMT-CFP-YFP). The average of five cells was analyzed for FRET efficiency.

ACKNOWLEDGMENTS

Electron microscopy was performed in the Cryo-EM core facility, Center for Structural Biology, University of Alabama at Birmingham. FRET experiments were performed in the FRET Core, High Resolution Imaging Facility, University of Alabama at Birmingham. We thank Kirill Popov for helpful comments and suggestions on the manuscript. This work was supported by National Institutes of Health Grant GM097052 to I.C.

REFERENCES

Adam JC, Pringle JR, Peifer M (2000). Evidence for functional differentiation among Drosophila septins in cytokinesis and cellularization. Mol Biol Cell 11, 3123–3135.

Balasov M, Huijbregts RP, Chesnokov I (2007). Role of the Orc6 protein in origin recognition complex-dependent DNA binding and replication in Drosophila melanogaster. Mol Cell Biol 27, 3143–3153.

Barral Y, Mermall V, Mooseker MS, Snyder M (2000). Compartmentalization of the cell cortex by septins is required for maintenance of cell polarity in yeast. Mol Cell 5, 841–851.

Bell SP (2002). The origin recognition complex: from simple origins to complex functions. Genes Dev 16, 659–672.

Bell SP, Dutta A (2002). DNA replication in eukaryotic cells. Annu Rev Biochem 71, 333–374.

Bertin A, McMurray MA, Grob P, Park SS, Garcia G 3rd, Patanwala I, Ng HL, Alber T, Thorner J, Nogales E (2008). Saccharomyces cerevisiae septins: supramolecular organization of heterooligomers and the mechanism of filament assembly. Proc Natl Acad Sci USA 105, 8274–8279.

Bertin A, McMurray MA, Thai L, Garcia G 3rd, Votin V, Grob P, Allyn T, Thorner J, Nogales E (2010). Phosphatidylinositol-4,5-bisphosphate promotes budding yeast septin filament assembly and organization. J Mol Biol 404, 711–731.

Bleichert F, Balasov M, Chesnokov I, Nogales E, Botchan MR, Berger JM (2013). A Meier-Gorlin syndrome mutation in a conserved C-terminal helix of Orc6 impedes origin recognition complex formation. Elife 2, e00882.

Casamayor A, Snyder M (2003). Molecular dissection of a yeast septin: distinct domains are required for septin interaction, localization, and function. Mol Cell Biol 23, 2762–2777.

Caudron F, Barral Y (2009). Septins and the lateral compartmentalization of eukaryotic membranes. Dev Cell 16, 493–506.

Chen S, de Vries MA, Bell SP (2007). Orc6 is required for dynamic recruitment of Cdt1 during repeated Mcm2–7 loading. Genes Dev 21, 2897–2907.

Chesnokov IN (2007). Multiple functions of the origin recognition complex. Int Rev Cytol 256, 69–109.

Chesnokov IN, Chesnokova ON, Botchan M (2003). A cytokinetic function of Drosophila ORC6 protein resides in a domain distinct from its replication activity. Proc Natl Acad Sci USA 100, 9150–9155.

Chesnokov I, Gossen M, Remus D, Botchan M (1999). Assembly of functionally active Drosophila origin recognition complex from recombinant proteins. Genes Dev 13, 1289–1296.

Chesnokov I, Remus D, Botchan M (2001). Functional analysis of mutant and wild-type Drosophila origin recognition complex. Proc Natl Acad Sci USA 98, 11997–12002.

Dobbelaere J, Gentry MS, Hallberg RL, Barral Y (2003). Phosphorylation-dependent regulation of septin dynamics during the cell cycle. Dev Cell 4, 345–357.

Duncker BP, Chesnokov IN, McConkey BJ (2009). The origin recognition complex protein family. Genome Biol 10, 214.

Dutta A, Bell SP (1997). Initiation of DNA replication in eukaryotic cells. Annu Rev Cell Dev Biol 13, 293–332.

Estey MP, Kim MS, Trimble WS (2011). Septins. Curr Biol 21, R384–387.

Fares H, Peifer M, Pringle JR (1995). Localization and possible functions of Drosophila septins. Mol Biol Cell 6, 1843–1859.

Field CM, al-Awar O, Rosenblatt J, Wong ML, Alberts B, Mitchison TJ (1996). A purified Drosophila septin complex forms filaments and exhibits GTPase activity. J Cell Biol 133, 605–616.

Field CM, Kellogg D (1999). Septins: cytoskeletal polymers or signalling GTPases? Trends Cell Biol 9, 387–394.

Ford SK, Pringle JR (1991). Cellular morphogenesis in the Saccharomyces cerevisiae cell cycle: localization of the CDC11 gene product and the timing of events at the budding site. Dev Genet 12, 281–292.

Founounou N, Loyer N, Le Borgne R (2013). Septins regulate the contractility of the actomyosin ring to enable adherens junction remodeling during cytokinesis of epithelial cells. Dev Cell 24, 242–255.

Haarer BK, Pringle JR (1987). Immunofluorescence localization of the Saccharomyces cerevisiae CDC12 gene product to the vicinity of the 10-nm filaments in the mother-bud neck. Mol Cell Biol 7, 3678–3687.

Hall PA, Russell SE (2012). Mammalian septins: dynamic heteromers with roles in cellular morphogenesis and compartmentalization. J Pathol 226, 287–299.

Hime GR, Brill JA, Fuller MT (1996). Assembly of ring canals in the male germ line from structural components of the contractile ring. J Cell Sci 109, 2779–2788.

Huijbregts RP, Svitin A, Stinnett MW, Renfrow MB, Chesnokov I (2009). Drosophila Orc6 facilitates GTPase activity and filament formation of the septin complex. Mol Biol Cell 20, 270–281.

Joberty G, Perlungher RR, Sheffield PJ, Kinoshita M, Noda M, Haystead T, Macara IG (2001). Borg proteins control septin organization and are negatively regulated by Cdc42. Nat Cell Biol 3, 861–866.

Johnson ES, Blobel G (1999). Cell cycle-regulated attachment of the ubiquitin-related protein SUMO to the yeast septins. J Cell Biol 147, 981–994.

Karpova T, McNally JG (2006). Detecting protein-protein interactions with CFP-YFP FRET by acceptor photobleaching. Curr Protoc Cytom Chapter 12, Unit12 17.

Kim HB, Haarer BK, Pringle JR (1991). Cellular morphogenesis in the Saccharomyces cerevisiae cell cycle: localization of the CDC3 gene product and the timing of events at the budding site. J Cell Biol 112, 535–544.

Kim MS, Froese CD, Estey MP, Trimble WS (2011). SEPT9 occupies the terminal positions in septin octamers and mediates polymerization-dependent functions in abscission. J Cell Biol 195, 815–826.

Kim MS, Froese CD, Xie H, Trimble WS (2012). Uncovering principles that control septin-septin interactions. J Biol Chem 287, 30406–30413.

Kinoshita M (2003). The septins. Genome Biol 4, 236.

Kinoshita M (2006). Diversity of septin scaffolds. Curr Opin Cell Biol 18, 54–60.

Kinoshita M, Field CM, Coughlin ML, Straight AF, Mitchison TJ (2002). Self- and actin-templated assembly of Mammalian septins. Dev Cell 3, 791–802.

Kinoshita M, Kumar S, Mizoguchi A, Ide C, Kinoshita A, Haraguchi T, Hiraoka Y, Noda M (1997). Nedd5, a mammalian septin, is a novel cytoskeletal component interacting with actin-based structures. Genes Dev 11, 1535–1547.

Lebedeva LI, Trunova SA, Omel'ianchuk LV (2000). [Genetic control of mitosis. Adaptive modifications of v158 mutation expression]. Genetika 36, 1348–1354.

Leipe DD, Wolf YI, Koonin EV, Aravind L (2002). Classification and evolution of P-loop GTPases and related ATPases. J Mol Biol 317, 41–72.

Liu S, Balasov M, Wang H, Wu L, Chesnokov IN, Liu Y (2011). Structural analysis of human Orc6 protein reveals a homology with transcription factor TFIIB. Proc Natl Acad Sci USA 108, 7373–7378.

Longtine MS, Fares H, Pringle JR (1998). Role of the yeast Gin4p protein kinase in septin assembly and the relationship between septin assembly and septin function. J Cell Biol 143, 719–736.

Longtine MS, Theesfeld CL, McMillan JN, Weaver E, Pringle JR, Lew DJ (2000). Septin-dependent assembly of a cell cycle-regulatory module in Saccharomyces cerevisiae. Mol Cell Biol 20, 4049–4061.

Low C, Macara IG (2006). Structural analysis of septin 2, 6, and 7 complexes. J Biol Chem 281, 30697–30706.

Machida YJ, Hamlin JL, Dutta A (2005). Right place, right time, and only once: replication initiation in metazoans. Cell 123, 13–24.

Mavrakis M, Azou-Gros Y, Tsai FC, Alvarado J, Bertin A, Iv F, Kress A, Brasselet S, Koenderink GH, Lecuit T (2014). Septins promote F-actin ring formation by crosslinking actin filaments into curved bundles. Nat Cell Biol 16, 322–334.

McMurray MA, Bertin A, Garcia G3rd, Lam L, Nogales E, Thorner J (2011). Septin filament formation is essential in budding yeast. Dev Cell 20, 540–549.

McTigue MA, Williams DR, Tainer JA (1995). Crystal structures of a schistosomal drug and vaccine target: glutathione S-transferase from Schistosoma japonica and its complex with the leading antischistosomal drug praziquantel. J Mol Biol 246, 21–27.

Mendoza M, Hyman AA, Glotzer M (2002). GTP binding induces filament assembly of a recombinant septin. Curr Biol 12, 1858–1863.
Mostowy S, Cossart P (2012). Septins: the fourth component of the cytoskeleton. Nat Rev Mol Cell Biol 13, 183–194.
Nagata K, Kawajiri A, Matsui S, Takagishi M, Shiromizu T, Saitoh N, Izawa I, Kiyono T, Itoh TJ, Hotani H, Inagaki M (2003). Filament formation of MSF-A, a mammalian septin, in human mammary epithelial cells depends on interactions with microtubules. J Biol Chem 278, 18538–18543.
Neufeld TP, Rubin GM (1994). The Drosophila peanut gene is required for cytokinesis and encodes a protein similar to yeast putative bud neck filament proteins. Cell 77, 371–379.
Pan F, Malmberg RL, Momany M (2007). Analysis of septins across kingdoms reveals orthology and new motifs. BMC Evol Biol 7, 103.
Prasanth SG, Prasanth KV, Stillman B (2002). Orc6 involved in DNA replication, chromosome segregation, and cytokinesis. Science 297, 1026–1031.
Saarikangas J, Barral Y (2011). The emerging functions of septins in metazoans. EMBO Rep 12, 1118–1126.
Sasaki T, Gilbert DM (2007). The many faces of the origin recognition complex. Curr Opin Cell Biol 19, 337–343.
Sellin ME, Sandblad L, Stenmark S, Gullberg M (2011). Deciphering the rules governing assembly order of mammalian septin complexes. Mol Biol Cell 22, 3152–3164.
Sellin ME, Stenmark S, Gullberg M (2012). Mammalian SEPT9 isoforms direct microtubule-dependent arrangements of septin core heteromers. Mol Biol Cell 23, 4242–4255.
Semple JW, Da-Silva LF, Jervis EJ, Ah-Kee J, Al-Attar H, Kummer L, Heikkila JJ, Pasero P, Duncker BP (2006). An essential role for Orc6 in DNA replication through maintenance of pre-replicative complexes. EMBO J 25, 5150–5158.
Sheffield PJ, Oliver CJ, Kremer BE, Sheng S, Shao Z, Macara IG (2003). Borg/septin interactions and the assembly of mammalian septin heterodimers, trimers, and filaments. J Biol Chem 278, 3483–3488.
Sirajuddin M, Farkasovsky M, Hauer F, Kuhlmann D, Macara IG, Weyand M, Stark H, Wittinghofer A (2007). Structural insight into filament formation by mammalian septins. Nature 449, 311–315.
Sirajuddin M, Farkasovsky M, Zent E, Wittinghofer A (2009). GTP-induced conformational changes in septins and implications for function. Proc Natl Acad Sci USA 106, 16592–16597.
Sprang SR (1997). G protein mechanisms: insights from structural analysis. Annu Rev Biochem 66, 639–678.
Takizawa PA, DeRisi JL, Wilhelm JE, Vale RD (2000). Plasma membrane compartmentalization in yeast by messenger RNA transport and a septin diffusion barrier. Science 290, 341–344.
Versele M, Thorner J (2004). Septin collar formation in budding yeast requires GTP binding and direct phosphorylation by the PAK, Cla4. J Cell Biol 164, 701–715.
Vrabioiu AM, Gerber SA, Gygi SP, Field CM, Mitchison TJ (2004). The majority of the Saccharomyces cerevisiae septin complexes do not exchange guanine nucleotides. J Biol Chem 279, 3111–3118.
Weirich CS, Erzberger JP, Barral Y (2008). The septin family of GTPases: architecture and dynamics. Nat Rev Mol Cell Biol 9, 478–489.
Wittinghofer A, Zent E (2014). Human septin isoforms and the GDP-GTP cycle. Biol Chem 395, 169–180.
Zent E, Vetter I, Wittinghofer A (2011). Structural and biochemical properties of Sept7, a unique septin required for filament formation. Biol Chem 392, 791–797.
Zhang Y, Gao J, Chung KK, Huang H, Dawson VL, Dawson TM (2000). Parkin functions as an E2-dependent ubiquitin- protein ligase and promotes the degradation of the synaptic vesicle-associated protein, CDCrel-1. Proc Natl Acad Sci USA 97, 13354–13359.